CHALMERS

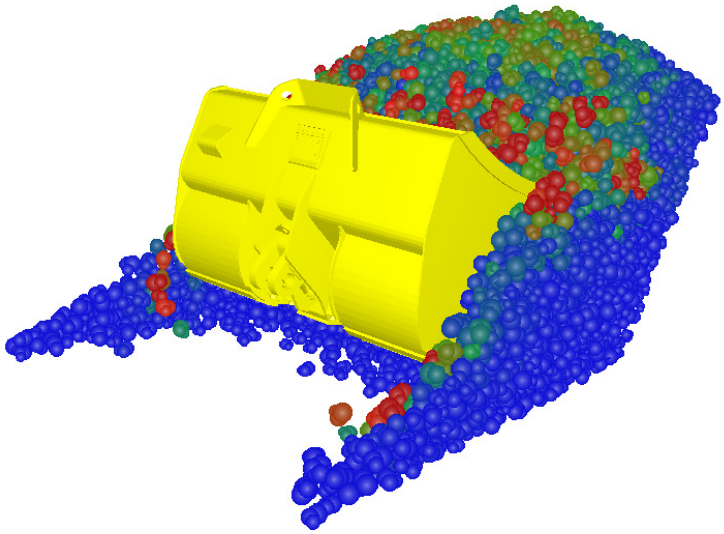

Optimization of Bucket Design for Underground Loaders

Master's Thesis in the International Master's programme Product Development

JONAS HELGESSON

Department of Product & Production Development
CHALMERS UNIVERSITY OF TECHNOLOGY
Göteborg, Sweden 2010

Optimization of Bucket Design for Underground Loaders

Master's Thesis in the Master's programme Product Development

JONAS HELGESSON

Department of Product & Production Development
CHALMERS UNIVERSITY OF TECHNOLOGY
Göteborg, Sweden 2010

Optimization of bucket design for underground loaders

Master's Thesis in the Master's programme Product Development

JONAS HELGESSON

ISSN 1652-8557
Department of Product & Production Development
Chalmers University of Technology
SE-412 96 Göteborg
Sweden
Telephone: + 46 (0)31-772 1000

Cover:
Bucket for underground loader in EDEM simulation with particle velocity displayed.

Chalmers reproservice
Göteborg, Sweden 2010

Optimization of bucket design for underground loaders
Master's Thesis in the Master's programme Product Development
JONAS HELGESSON
Department of Product & Production Development
Chalmers University of Technology

Abstract

An optimized bucket design is important for increasing productivity and loading performance for underground loaders. Design theories are today difficult to evaluate due to lack of verification methods. Later year's development of simulation software and computers has made it possible to verify the design by simulating the loading process. The purpose with this thesis has been to both develop and use a simulation model of the loading process for one of Atlas Copco's underground loaders.

A simulation model was developed in the program EDEM. EDEM uses the Discrete Element Method for simulating granular materials, which in this case was blasted rock. Factors such as particle flow, particle compression and loading setup adds complexity and uncertainty to the task. Nevertheless was a model that was able to detect force variations from small design changes developed.

The tractive effort is the horizontal force the loader can generate. This the critical factor when loading rocks, with use of EDEM different bucket designs could be evaluated by studying the horizontal force in the simulations. The simulation model was compared with practical tests.

The edge thickness of the bucket lip was the individual design parameter that had the largest influence on the horizontal force; a thin edge generated lower force. In general a bucket with sharp and edgy shape gave lower forces. The attack angle (bottom angle) had low influence on the horizontal force.

Key words: Bucket design, bucket filling, DEM simulation, underground loader

Table of Contents

Preface

The purpose of this thesis is to develop and use a simulation model of the loading process for buckets of underground loaders. The thesis was initiated both by Atlas Copco Roc Drills AB (Atlas Copco) and Chalmers University of Technology. The project has been financed by Atlas Copco and performed at the department for underground loaders in Örebro, Sweden. The time frame for this project has been January 2010 – June 2010.

The student performing the work has been Jonas Helgesson. Supervisor from Atlas Copco has been Stefan Nyqvist and assistant supervisors have been Anders Fröyseth, Andreas Nord and Morgan Norling. Examiner and supervisor from Chalmers has been senior lecturer Göran Brännare from the Department of Product and Production Development, Chalmers University of Technology, Göteborg, Sweden.

I would like to thank all in the department for underground loaders at Atlas Copco for their support and help, especially Stefan Nyqvist, Anders Fröyseth, Martin Hellberg, Kjell Karlsson and Andreas Nord. I would also like to thank my supervisor at Chalmers, Göran Brännare.

Örebro 23rd of June 2010

Jonas Helgesson

Notations

deg	Degrees
CAE	Computer Aided Engineering
COR	Coefficient of Restitution
DEM	Discrete Element Method
ECTS	European Credit Transfer System
EDEM	Engineering Discrete Element Method
FEM	Finite Element Method
G	Shear modulus
GET	Ground Engagement Tools
LHD	Load Haul Dump
MBS	Multi Body Simulation
mm	Millimetre
rpm	Revolutions per minute
s	Seconds
ST	Scoop Tram
α	Inclination of soil pile
β	Inclination of the initial phase of trajectory
Δt	Time step
δ	Attack angle
μ_s	Static Friction
μ_r	Rolling Friction
ν	Poisson's ratio

1 Introduction

1.1 Project Background

This report is the result of a master's thesis conducted at Atlas Copco Rock Drills AB (Atlas Copco) in Örebro during spring 2010. It covers 30 ECTS (European Credit Transfer System) points.

Atlas Copco wants to investigate the design of the buckets for underground loaders used for loading rocks. Within the company there are some theories and knowledge about how the design of the bucket influences the loading performance, but the lack of verification of this information makes it difficult to optimize the design.

Development of simulation software and computers has made it possible to simulate the loading process of a bucket, this development has realized possibilities to gain knowledge in this area.

A computer software named EDEM (Engineering Discrete Element Method) has successfully been used for simulations of rock crushing at Chalmers. Other actors have used EDEM for bucket simulations, this emphasizes the possibility to use EDEM for simulating the loading process.

1.2 Company Background

Atlas Copco AB is a Swedish company founded in 1873. Atlas Copco is a supplier of industrial productivity solutions and the product portfolio cover a wide range of areas; compressed air equipment, generators, construction and mining equipment, industrial tools and assembly systems. In total, Atlas Copco had 31 000 employees in 2009, a revenue of 64 BSEK and was active in more than 170 countries.[1]

An American company, Wagner Mining Equipment Company, was bought by Atlas Copco 1989 [13]. Wagner manufactured underground loaders and trucks. After Wagner's merge with Atlas Copco, Atlas Copco was able to supply equipment for both bursting, loading and transportation of ore. Wagner's activity was 2005 moved to Örebro where the underground division is centralized today, both development and manufacturing of mining equipment takes place in Örebro. All loaders and trucks are today marketed under the Atlas Copco brand.

1.3 Problem Description

To maximize efficiency it is important get a fully filled bucket in one loading cycle. The tractive effort (horizontal force) is a critical factor related to the bucket filling. By reducing forces with an efficient bucket design, time, wear and energy consumption will be reduced. Sometimes the bucket is not fully loaded in one cycle and the process has to be repeated, this should be avoided.

1.4 Purpose

The purpose of this thesis is to develop a simulation model of the loading process for buckets of underground loaders. The influence from different design parameters will then be investigated, to generate guidelines for the design of the next generation of buckets at Atlas Copco.

Another aspect of the thesis is to investigate the potential of the computer software and look for more areas of application than only design of buckets.

In an educational view the purpose of this thesis is to gain knowledge in the following areas: The discrete element method, working with simulation programs and get an understanding for the relation between reality and a virtual simulation.

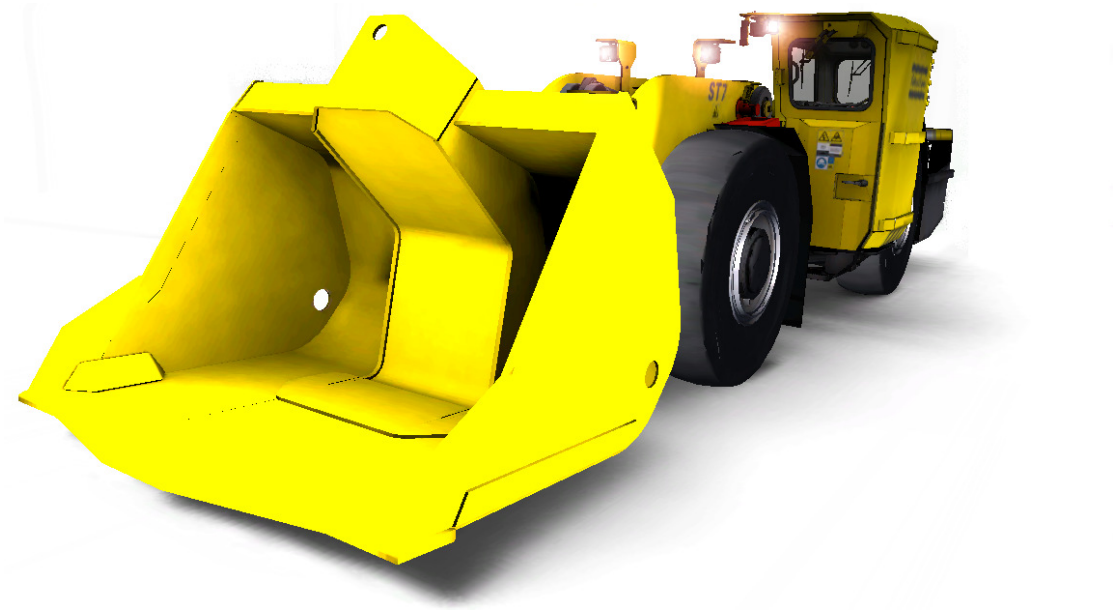

Figure 1: Atlas Copco's scooptram ST7.

1.5 Limitations

The main focus will be on investigating the bucket design. One moving trajectory for the bucket will be defined and used in the simulations. The thesis will focus on Atlas Copco's scooptram ST7, see Figure 1, with a standard bucket. No full scale testing of modified buckets will be performed. Other design aspects, such as wear resistance and rigidity will not be prioritized.

If time is available also other sizes of loaders will be investigated.

1.6 Method

A simulation model of the loading process for buckets of underground loaders will be developed. The model will then be used to investigate which parameters that affect the loading result. The final step will be to optimize the loading parameters to achieve an efficient loading process. Program to be used for this task is EDEM, also ADAMS can be necessary to use. Real tests will be performed to analyze today's existing buckets and to generate result to use for verification of simulations.

Existing knowledge on the market and within Atlas Copco will be collected and compiled.

2 Theory

2.1 Machine

The Atlas Copco ST7 is a LHD (Load-Haul-Dump) machine and is used for loading blasted rock material in mines. In general it works as a normal wheel loader, the difference is the compact design to be able to navigate in narrow underground paths and the high loading weight capacity due to the heavy loading material. Compared to a wheel loader the operator's visibility is much more limited. It is difficult for the operator to get a good view of the material flow into the bucket during loading. For technical specification of ST7 see Appendix A1.

2.2 Working Cycle

For mining process in both steep and flat orebodies, see Appendix A2, the working cycle for underground loaders is similar.

The loader approach the pile with the boom, buckets lifting arm, in the lower position and the bucket lip is horizontal to ground. The machine is primarily built for executing the loading process with the boom in the lowered position, but operators often raise the boom during loading to get a better bucket filling [16]. The loader is driven into the pile until the wheels are getting close to start to slip (slipping point) [16]. At this stage the operator starts to tilt the bucket (rotates around the attachment axis), see Figure 2. The tilting increase the vertical force on the wheels and decrease the horizontal force needed [21]. The bucket is loaded by continuously driving into the pile and tilting the bucket at the same time. When it is fully tilted the bucket is loaded and the machine retracts from the pile.

Figure 2: Bucket is loaded with boom in lower position.

With the bucket in tramming position, see Figure 3, the rock is transported and unloaded into a truck, see Figure 4, or in some cases into a pit.

Figure 3: The rock is transported to truck with bucket in tramming position.

Figure 4: The loader is unloading the rock into a mine truck.

2.3 Loading Material

In mining the properties of the material varies between each loaded bucket [16]. The density of the rock varies with the mineral content in the rock and the kind of waste material, e.g. greystone or granite. Since the composition of the material varies over the mountain the density will vary. Normally an average density is specified for a mine, but this value does not give the whole truth about the material density.

When the rock is blasted it is divided into small pieces with a large variation of size and shape. The differentiation is dependent of rock material, explosive charge and placement of the explosives [16]. The large variation in size and shape makes it difficult to specify an average material for simulation.

Figure 5: Material used for performing loading tests, the yellow ruler has a length of 50cm.

2.4 General Bucket Background

Compared to standard wheel loaders the bucket equipped on underground loaders has a more robust design, see Figure 6 and Figure 7. The more robust design for underground loaders is required due to intensive operation conditions in mines. Severe wear on the bucket during operation leads to a bucket having a lifetime of approximately 8000h, the lip is usually replaced after 500-1500h. To replace a worn out bucket is an expensive cost for mining companies.

The hard and aggressive loading material is difficult to penetrate with a bucket. Low penetration force is therefore a prioritized area when designing buckets for mining industry.

The height and width of the bucket is limited by the machine size. The bucket shall be 2-3dm wider than the machine and not reach above the machine body.

Figure 6: Volvo wheel loader bucket.

Figure 7: ST7 GIII standard bucket.

2.5 Bucket Loading Theory

Figure 8 and Figure 9 seen below are taken from a study performed by Coetzee and Els [4]. The bucket in the study was a dragline bucket and the test results are from a down scaled test. The test was done using corn as granular material. Figure 9 shows the percentage of the total drag force during the loading cycle that acts on each part of the bucket. Test conditions in this study are different compared to actual conditions for an underground loader. However, several interesting observations can be made. During the entire cycle 25-30% of the drag force acted on the lip, this makes the design of the lip important. When material reach the rear parts of the bucket, between 300-600mm see Figure 9, these parts become a larger part of the drag force. There were no side plates on the bucket used in the test.

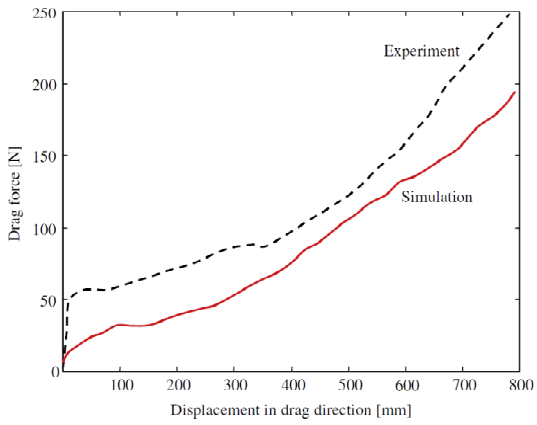

Figure 8: Measured forces for dragline bucket.

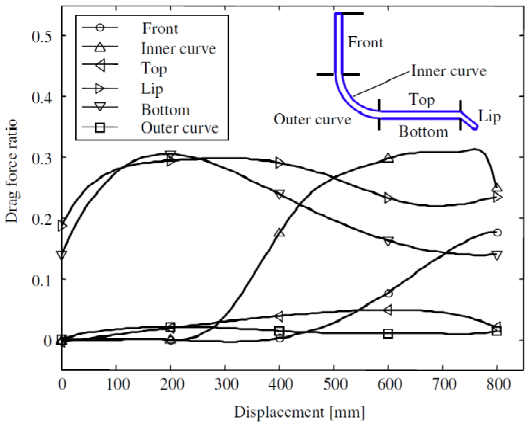

Figure 9: Forces on each bucket part.

Maciejewski [7] did a study where the aim was to optimize the digging process and bucket trajectories. It was shown that the most energy efficient bucket is the one where the pushing effect on the back wall is minimized.

Esterhuyse [5] and Rowlands [9] investigated the filling behaviour of scaled dragline buckets. The bucket with the shortest fill distance was found to produce the highest peak in drag force. When filling an underground loader the peaks in drag force are critical since at these points the machine start to slip.

An interesting design parameter on the bucket is the attack angle (bottom angle). The effects of the attack angle have been studied by Maciejewski [7]. Attack angles of 5˚, 15˚ and 30˚ were tested, the result is seen below in Figure 10 and Figure 11. The bucket was moved into the pile horizontally.

β - inclination of the initial phase of trajectory (equal to 0˚ in test)

α - inclination of soil pile (equal to 50˚ in test)

δ - attack angle

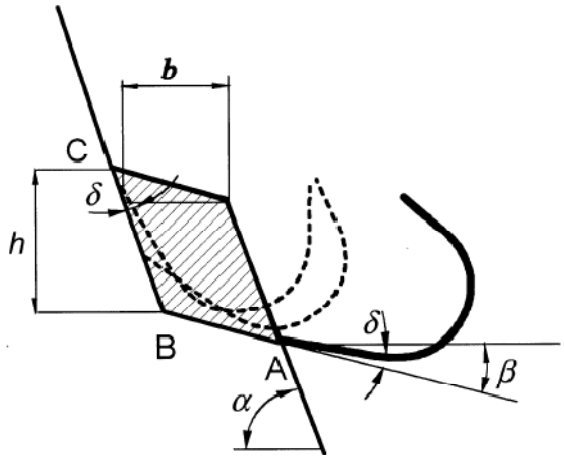

Figure 10: Scheme of rotational cycle.

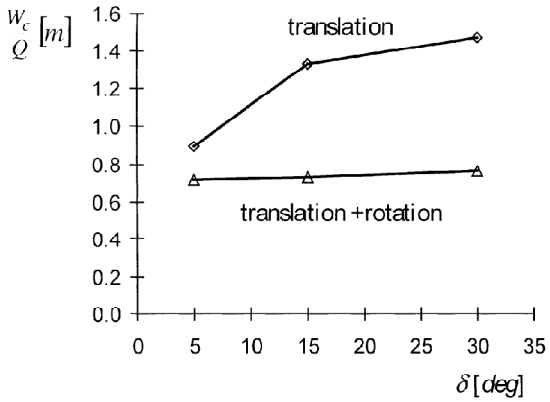

Figure 11: Specific energy versus the attack angle for different bucket motion.

When only a translational motion was applied to the bucket the total energy for loading increased dramatically with a higher attack angle, see Figure 11. But when a rotational motion was added to the bucket the change in energy was close to zero.

Atlas Copco's loaders are using a rotational motion. According to Maciejewski's study a variation of the attack angle, on Atlas Copco's bucket, will have a low impact on loading energy.

2.6 Description of Discrete Element Method

The Discrete Element Method (DEM) is a computational method used for calculating the behaviour of e.g. a granular material. In the following text a brief introduction is presented.

In modelling of a ordinary engineering problem a number of well defined components normally are involved. The behaviour of each component is either known or can be calculated. The problem is solved by using mathematical functions that describes the individual components behaviour and their interactions [6]. This is a common approach to use for solving mechanical problems.

For more complex problems, e.g. components of flexible material, the finite element method (FEM) is used. FEM divides the component into small elements. The behaviour of each element is approximated by simple mathematical description with finite degrees of freedom. With use of FEM a correct behaviour of the component can be calculated. FEM is used for individual components/bodies with known boundary conditions.

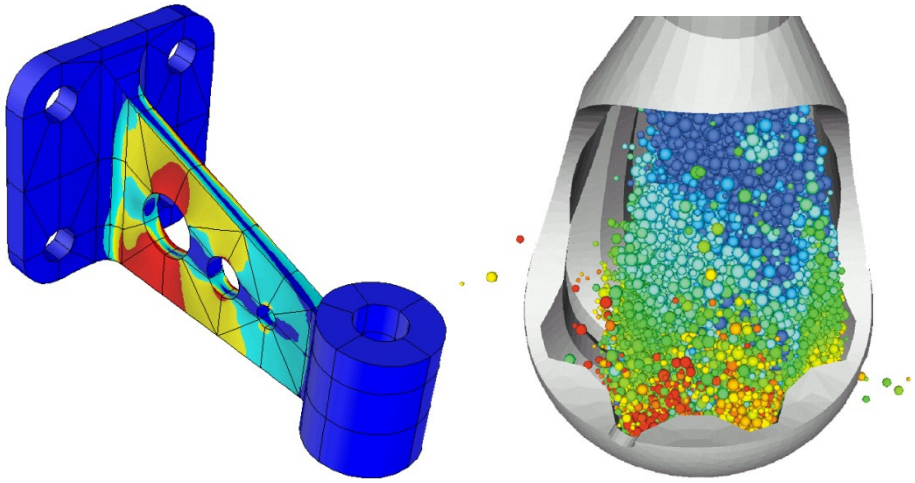

Figure 12: Left, typical FEM application. Right, typical DEM application.

A problem, such as calculating the motion of a pile of rock, generates too complicated computations if every stone is taken into account. The FEM approach is based on that the material remain in the same position throughout the simulation and is there for not suitable to use for simulations of a granular material.[6]

The most common method to use for analysing granular material, e.g. a pile of rock, is DEM. DEM is treating the rock pile as a collection of independent units, each stone in the pile is an individual unit and each stone is free to move according to its forces. The behaviour of the stones is calculated from contact between them, velocity and deformability. With use of DEM a good approximation of blasted rock can be reached if the problem dimensions, material properties and boundary conditions are properly defined [6]. Compared to FEM, DEM is used for units in motion and FEM is focused on material deformation. Typical examples of FEM and DEM are displayed in Figure 12.

2.6.1 DEM Program Theory

A DEM program involves a lot of complicated computations. A simplified description of the computations process follows below:

A timestep, Δt, is defined in the DEM program. Δt specify with what interval the position and motion of the particles should be recalculated. The following loop (1-5) is run every timestep in the DEM program and describes more into detail how a DEM program works.

1. Position and motion of each particle is registered
2. Particle contact detection
   The problem domain is divided into a cubical mesh. Position of particles in the same "cube" are compared to track if intersection appear.
3. Contact zones are determined
4. Intersection distances are determined

5. Forces are determined

   The forces are calculated with use of all previous collected data about motion and contact, together with material and material interaction properties.

It is of importance that the timestep is selected correctly to avoid large intersections which will result in large unrealistic forces. The simulation time is related to the timestep, a smaller timestep generate longer run times. [12]

3 Execution

3.1 Practical Test of Scoop Loading

A practical loading test was performed in connection to Lovisagruvan situated in Västmanland, Sweden. The test was performed at surface level, above the mine. Two ST7 machines were used and two different buckets, GII and GIII (see Figure 13), was mounted on the machines. The buckets had equal capacity, built for a material density of 2.2ton/m³ and had a volume of 3.1m³.

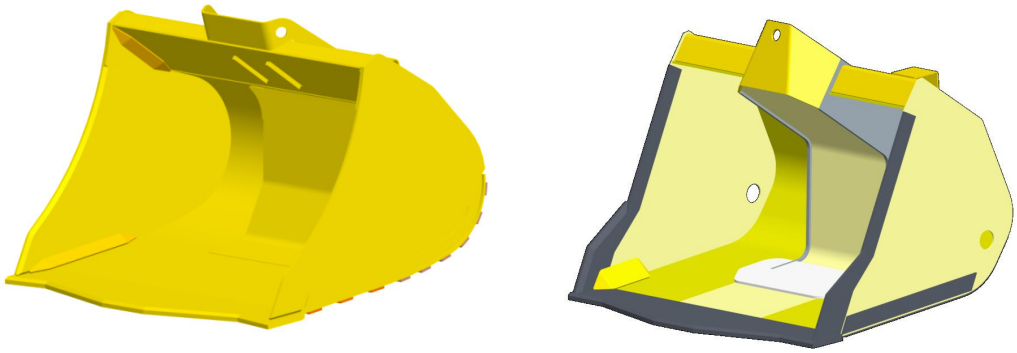

Figure 13: ST7 GIII bucket, left, and ST7 GII bucket, right.

A pile of greystone, with a density of approximately 1,6ton/m³, was built up to use for the loading test, Figure 14. The material had an average diameter between 10 to 15cm. Compared to a normal loading material in a mine this was more loosened up and the density was lower, which make it an easy material to load.

Two types of loading procedures were tested. One where efficient loading was prioritized i.e. a combination of short loading cycle and high filling grade was the aim. In the second test maximum filling was prioritized. Each test was performed 10 times with both buckets. The result was generated by measuring the weight of the load and the time for performing a loading cycle. Other factors were also taken into account, the operator's opinion and the visual image of the test.

An additional test was performed where the penetration distance of the bucket was measured. The loader was driven into the pile until the wheels started to slip, without any tilting of the bucket

Figure 14: Practical test setup.

3.2 Simulation Model in EDEM

EDEM (Engineering Discrete Element Method) is a program developed in Scotland by the company DEM Solutions. The program uses DEM to simulate granular materials in motion. EDEM models the material as a group of individually particles that interact only at the inter-particle contact points. [11]

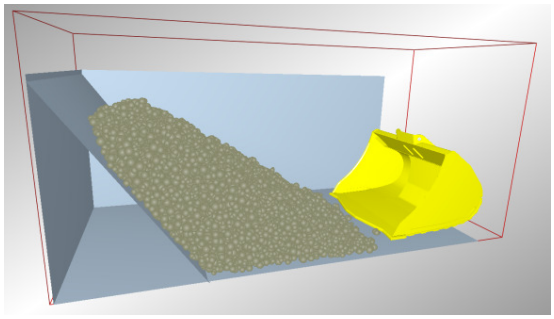

Figure 15: Simulation setup in EDEM.

With EDEM exactly the same loading procedure in the same rock pile can be performed. Different bucket designs can then be simulated and resulting data can be used to optimize the bucket design. The simulation setup in EDEM is seen in Figure 15.

3.2.1 Selecting Parameters in EDEM

The material is defined by a number of parameters in EDEM, divided into material and interaction properties. The interaction is defined as between particles and between particles and bucket. The main problem with DEM simulations is to specify the interaction properties so the particles behave in the same way as in reality [3].

The shape of the particles is defined by using multiple spheres that are bonded together to give a realistic outer shape. The particle seen in Figure 16 was the one used in simulations.

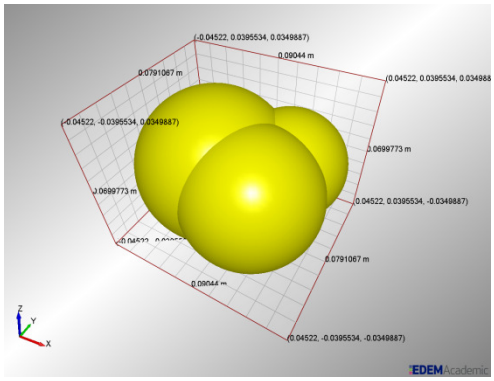

Figure 16: Particle used in simulations.

Since the material properties are different in every mine, properties have been selected to represent an average material.

Material specific properties can be taken directly from literature, where as the interaction parameters are more difficult to specify. Interaction parameters are confirmed by visually verify that the simulation behaves as in reality.

Information about simulation parameters has been collected from several sources [10, 11, 14, 15] and values shown in Table 1 have been chosen for the simulation model.

Table 1: Material parameters used in EDEM.

Material parameters			
Material	Rock	Steel	Ground
Poisson's ratio, ν	0.25	0.3	0.25
Shear modulus, G [MPa]	240	7 000	1
Density [kg/m³]	3000	8000	1000
Particle diameter [mm]	70-120	-	-
Interaction parameters			
Interaction materials	rock-rock	rock-steel	rock-ground
Coefficient of restitution, COR	0.2	0.2	0,2
Static friction, μ_s	0.65	0.4	0.5
Rolling friction, μ_r	0.1	0.05	0.05

Material parameters:

Shear modulus, G

The value of shear modulus (stiffness) have a high impact on the calculation time for the simulations in EDEM, a high shear modulus of the granular material generates a very long calculation time. Also a high shear modulus can give unrealistic forces when the material is exposed for compression forces [17]. To save calculation time and avoid high force peaks a reduction of the shear modulus is preferred. As long as the shear modulus is high enough to prevent any large interpenetration of particles the simulation will generate a reliable result. [8]

24 000MPa is seen as an appropriate value for shear modulus of rock but in the simulations a value of 240MPa has been used. According to DEM Solutions the shear modulus can normally be reduced 100 times.

Density

In EDEM the density is specified for solid material, for Atlas Copcos buckets the density are defined for broken material. Solid material expands approximately about 1.5-1.7 times when it becomes broken [16]. In the simulation a standard bucket that is designed for a maximum density of 2.2ton/m³ is used and the bulk material have a solid density of 3ton/m³ which generates a density of 1.875ton/m³ for broken material with an expansion factor of 1.6.

Interaction parameters:

Coefficient of Restitution, COR

The COR value describes the bounciness of the particles or the inverse of the damping. An appropriate COR value is 0.25 for rock-rock and 0.3 rock-steel. A lower COR value gives lower force peaks and a more stable simulation [19], because of this the COR value was slightly reduced to 0.2 for both rock-rock and rock-steel.

Static Friction, μ_s. Rolling Friction, μ_r

The friction coefficients are exaggerated compared to the real values. This is because the particles in EDEM have a smooth and rounded surface. A real stone has waviness on the surfaces and also small irregularities. To get the almost round particles to behave as realistic stones the friction coefficients are increased.

3.2.2 Defined Motion Path in EDEM

CAD models of buckets were imported into EDEM. The models are given a specified motion that digs through a pile of granular material that consists of 11 000 particles. The motion is defined by speed and acceleration for a limited time period in the program. Rotational velocity is also added around the buckets rotation point.

The bucket follows a specified motion path that is fixed through the rock pile. When peaks in forces appear on a real bucket small motions occur due to tire deflection, cylinder compression or motion slowdown. This kind of parameters are not possible to add in EDEM. To get a more realistic behaviour, a model of the loader needs to be built in a separate computer program, e.g. ADAMS, and then imported into EDEM. This is a complicated and time consuming task, which is not covered in this thesis.

The motion cycle used in EDEM is defined by studying the exact motion from the practical test session. The defined cycle can be seen in Appendix A3. Figure 17 shows snapshots of the cycle at different time steps.

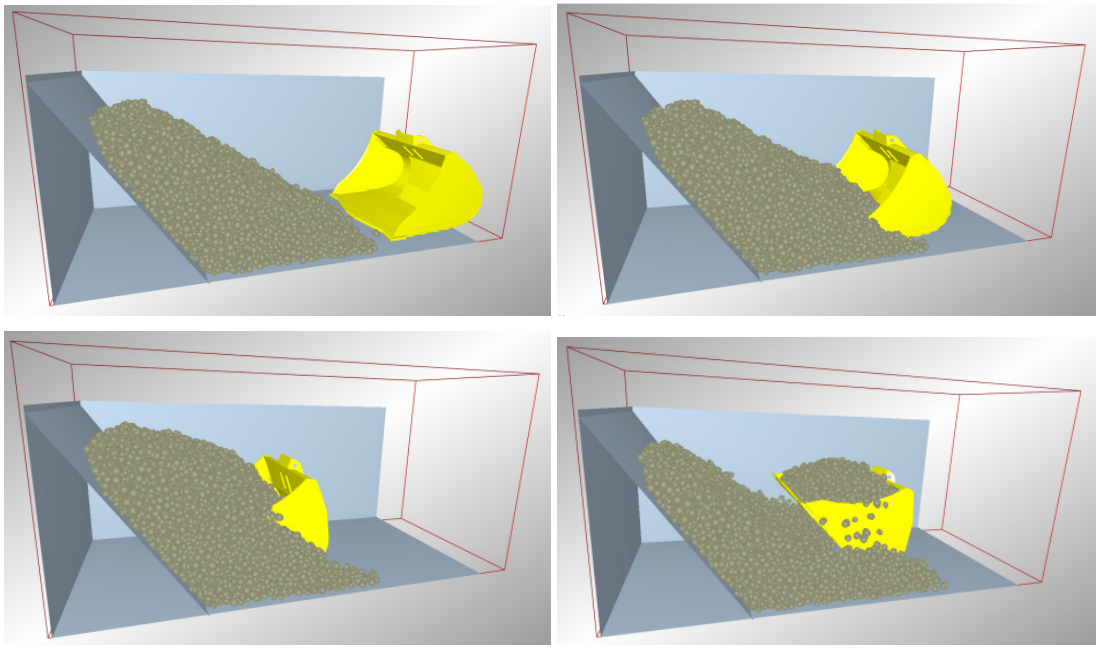

Figure 17: Simulation cycle shown after 0, 4, 8 and 11s.

3.2.3 Bucket Design Parameters

By studying the design parameters separately, an optimum value for each parameter is hopefully found. The design parameters are assumed to act independent of each other which makes this method reliable.

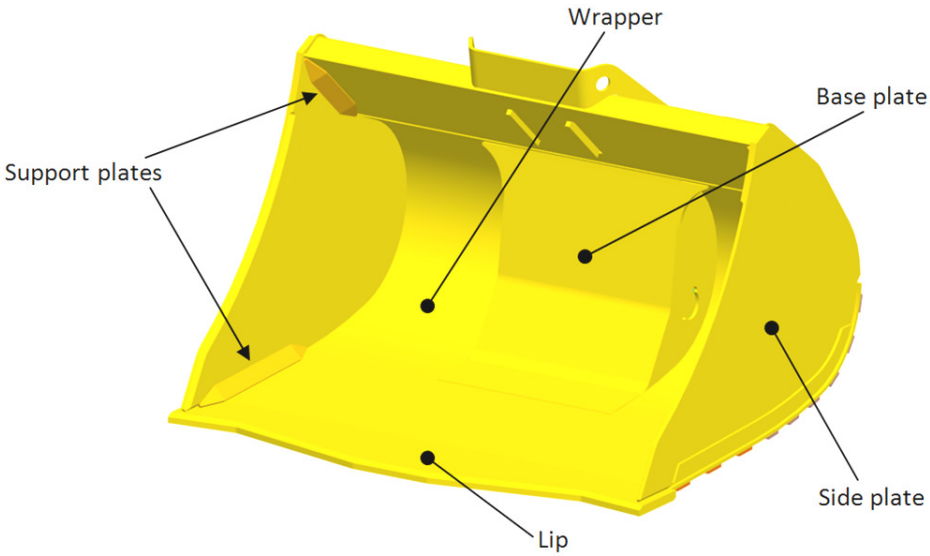

Figure 18: Denomination of bucket parts.

Design parameters selected for investigation are: Lip angle, lip chamfer, lip profile, attack angle (bottom angle), base plate design, side plate angle, side plate profile and support plate. Parameters are described in Figure 18 to Figure 23.

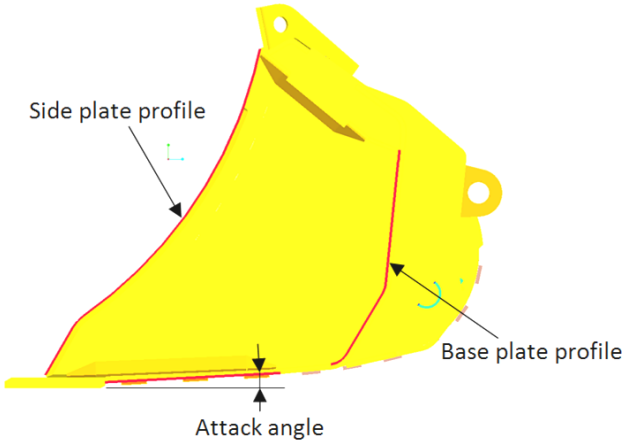

Figure 19: Side plate profile, attack angle and base plate profile.

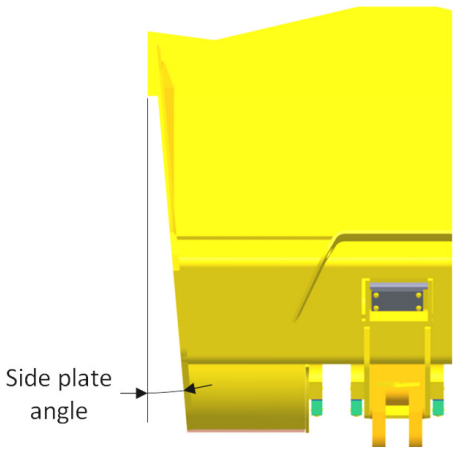

Figure 20: Side plate angle

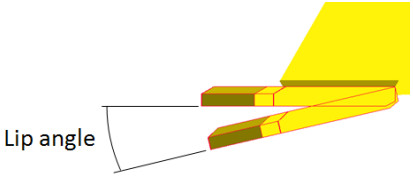

Figure 21: Lip angle

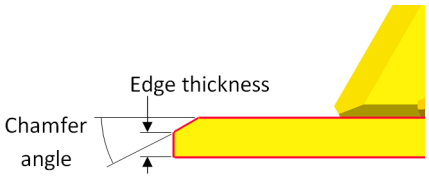

Figure 22: Chamfer angle and edge thickness.

Figure 23: Lip profile

The base plate exists to give space for bucket attachment. Some competitors has a design without base plate. This gives a smooth inner design but the disadvantage is that the rotation point is moved backwards and the centre of mass is moved forward.

3.2.4 EDEM Setup Description

Two different paths of movement in the loading cycle has been used. One path where the bucket lip follow the ground and one path where the bucket path is 300mm above the bottom plate, see Figure 24 and Figure 25.

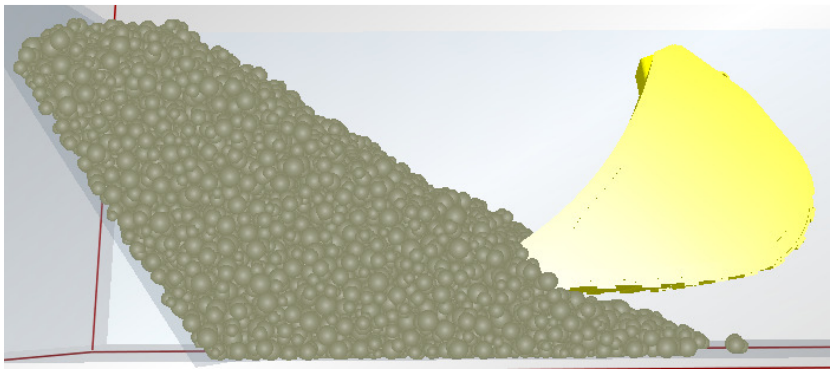

Figure 24: High simulation cycle.

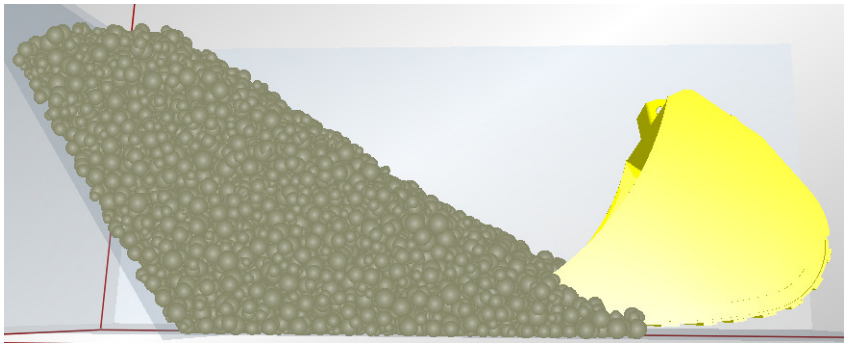

Figure 25: Low simulation cycle.

Unrealistic large compression forces appear in some simulations in the particles between the bucket and the ground. This is a software related problem [17]. One of the reasons to this is that no crushing of stones occurs in EDEM.

Two different simulation setups give a possibility to evaluate the reliability of the simulation results. If the two simulations show converging results it is shown that the simulations are generating reliable results.

An angled plate has been added in the corner of the box. The reason for this is to reduce the total amount of particles, which in turn reduces the calculation time. Another reason is to avoid unrealistic compression forces of the particles that got stuck in the corner. See angled plate in Figure 25.

The width of the simulation box is 2800mm and the maximum width of the bucket is 2230mm. This gives a span of 285mm on each side of the bucket, see Figure 26. The side boundaries are periodic, which means that a particle can pass through the wall at one side and come out from the wall at the other side. This configuration seem to give a realistic behaviour of the particles outside the side plates.

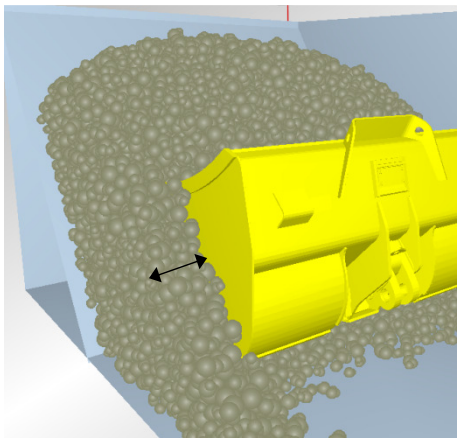

Figure 26: The span between side boundary and bucket is 285mm.

One simulation cycle takes 2.5 hours to simulate.

3.2.5 Evaluation of Output from EDEM Simulations

The goal with simulations was to design a bucket that was easy to fill. In reality a good measure of this is the amount of load in the bucket after a performed loading cycle. In EDEM all buckets follow the same path which gives almost equal load, instead differences are seen on the forces acting on the bucket.

The horizontal force is of large interest since it is in direct relation to the tractive effort required for executing the loading cycle. A large vertical force increases the front wheel grip and gives the machine a higher tractive effort. The forces are presented in graphs, see Figure 27, and the average force over time was calculated and used for comparison. The loading cycle is 11s but only the average force for the first 7s was used as a comparison value. During the first 7s the buckets penetration capability is important, to use the result from the complete cycle add more insecurity to the result.

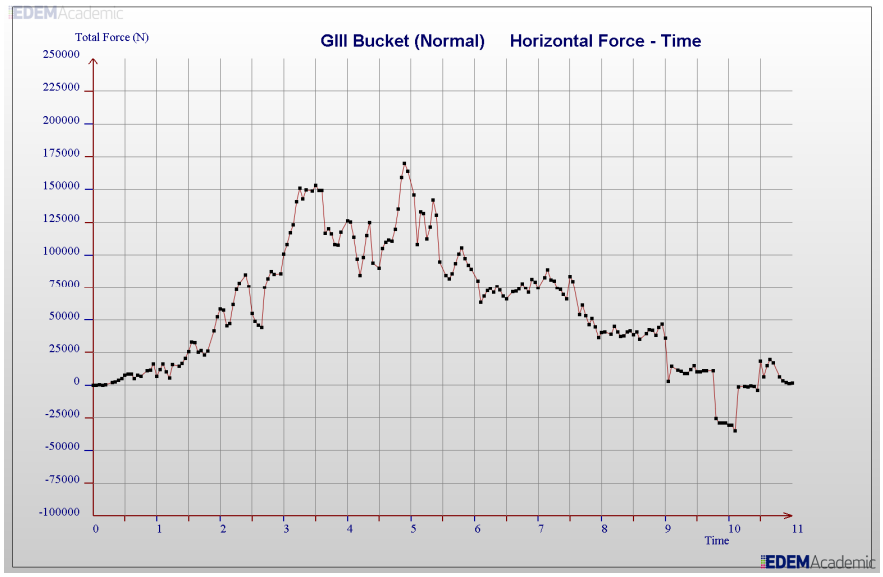

Figure 27: Graph of horizontal force for GIII bucket in low simulation setup.

The torque around the buckets rotation point can be plotted, this torque is in relation to the buckets breakout force.

With a function in EDEM the weight of the load in the bucket was measured, see Figure 28, this made it possible to relate the forces to the amount of load.

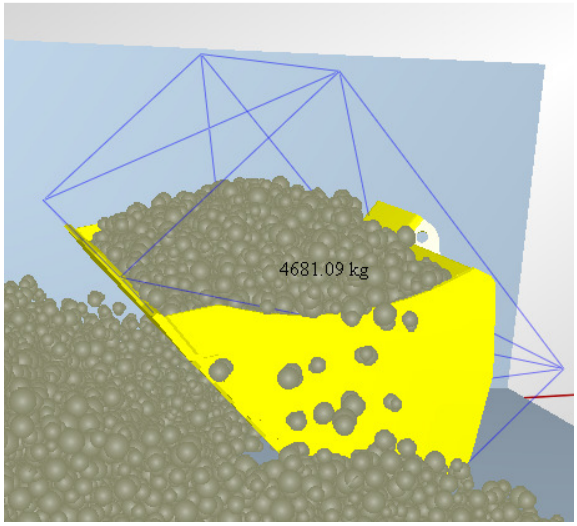

Figure 28: Material weight for loaded bucket displayed in EDEM.

Multiple runs of the same simulation setup (equal bucket and pile) generated a result variation. This was due to a large timestep [17]. Because of this 4 runs of each simulation setup was completed and an average result was calculated. The large timestep makes the particles take different flow paths in each simulation, this is good for getting a more reliable result. The large timestep also generates high force peaks which lower the accuracy in the result outcome. A small timestep give long simulation runtime.

4 Results

4.1 Outcome of Practical Test

4.1.1 Loading Test

A difference between the GIII and the GII bucket was possible to distinguish in the loading result. The newly developed bucket, GIII, was easier to fill compared to the older, GII. GII had a heap that was displaced in the front end of the bucket and in the rear part of the bucket there was most often an empty gap that led to a lower filling grade. In 85% of the loading cycles GIII had a good filling, compared to only 30% for GII. GIII had also a slightly faster loading time.

During the loading cycle the rpm was measured and the pressure in the hoist and dump cylinders. The rpm value gave a rough estimation of the machines tractive effort into the pile. The rpm value did vary between loading cycles and was sometimes fluctuating and sometimes constant during bucket filling. A rough estimation is that the upper level during the loading was 1700rpm, which can be translated to a tractive effort of 110kN, see Figure 70 in Appendix A1 for explanation.

4.1.2 Penetration Test

The result of the penetration test was that the GIII bucket had a 10-20% deeper penetration. But since the pile shape seemed to has a large impact on the result no conclusions were drawn from this test.

4.2 Investigating the Influence of Design Parameters

4.2.1 GII Bucket

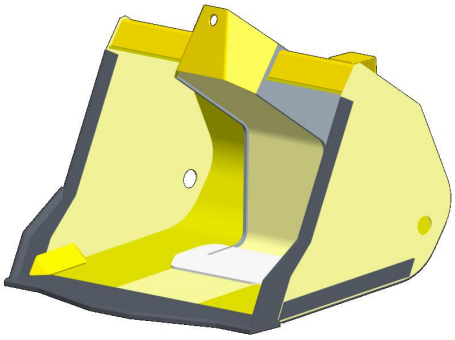

Figure 29: GII

Load	4516kg
Horizontal force per kg load	16.6N/kg
Vertical force per kg load	-3.1N/kg
Horiz. force compared to GIII - low setup	+4.3%
Horiz. force compared to GIII -high setup	+2.2%

The old GII Bucket was less efficient to fill compared to the Normal GIII Bucket. This result corresponds with the practical test. The load was 200kg lower than with Normal Bucket.

4.2.2 Lip Profile

Figure 30: GIII, Normal

Load	4720.1kg
Horizontal force per kg load	15,9N/kg
Vertical force per kg load	-3.4N/kg
Horiz. force compared to normal	0.0%
Horiz. force comp. - high setup	0.0%

Figure 31: V/straight

Load	4720.5kg
Horizontal force per kg load	15.7N/kg
Vertical force per kg load	-3.74N/kg
Horiz. force compared to normal	-1.6%
Horiz. force comp. - high setup	-0.9%

Figure 32: Straight

Load	4667.3kg
Horizontal force per kg load	16.1N/kg
Vertical force per kg load	-2.7N/kg
Horiz. force compared to normal	+1.1%
Horiz. force comp. - high setup	+3.0%

Figure 33: M-extreme

Load	4664.3kg
Horizontal force per kg load	15,9N/kg
Vertical force per kg load	-3.4N/kg
Horiz. force compared normal	+0.1%
Horiz. force comp. - high setup	-1.7%

Figure 34: V- 10deg

Load	4791.1kg
Horizontal force per kg load	16.1N/kg
Vertical force per kg load	-2.4N/kg
Horiz. force compared to normal	+1.4%
Horiz. force comp. - high setup	+1.3%

Figure 35: V- 16deg

Load	4877kg
Horizontal force per kg load	15.2N/kg
Vertical force per kg load	-4.3N/kg
Horiz. force compared to normal	-4.7%
Horiz. force comp. - high setup	+0.8%

Figure 36: V- 21deg

Load	4930.8kg
Horizontal force per kg load	15,8N/kg
Vertical force per kg load	-3.7N/kg
Horiz. force compared to normal	-1.0%
Horiz. force comp. - high setup	-1.5%

V/straight and V-21deg has a slightly smaller horizontal force than normal M-shaped lip, both for high and low test cycle. The low horizontal force for V-16deg low setup can probably be seen as a simulation variation.

Graphs of horizontal and vertical force for the GIII bucket are shown in Appendix A4.

4.2.3 Base Plate Profile

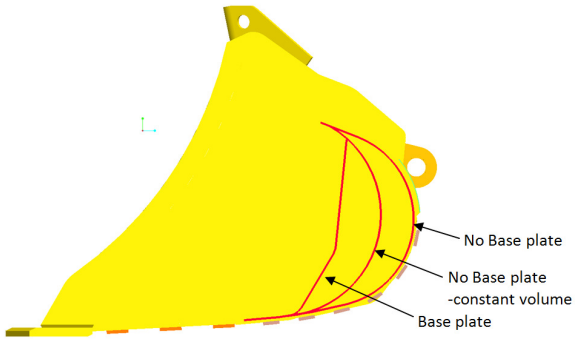

Figure 37: Inner profile description.

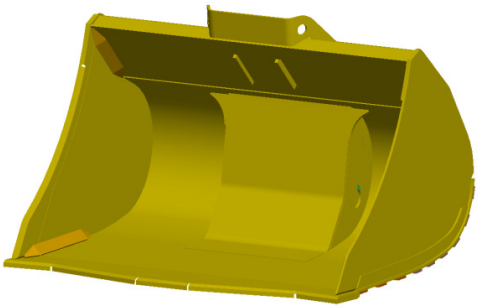

Figure 38: Base plate (GIII, Normal)

Load	4720.1kg
Horizontal force per kg load	15,9N/kg
Vertical force per kg load	-3.4N/kg
Horiz. force compared to normal	0.0%

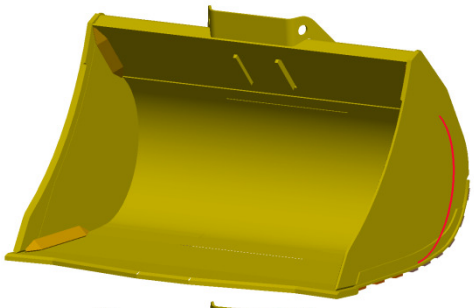

Figure 39: No base plate constant volume

Load	4717.8kg
Horizontal force per kg load	16.2N/kg
Vertical force per kg load	-2.5N/kg
Horiz. force compared to normal	+1.7.%

Inner profile of wrapper highlighted in figure.

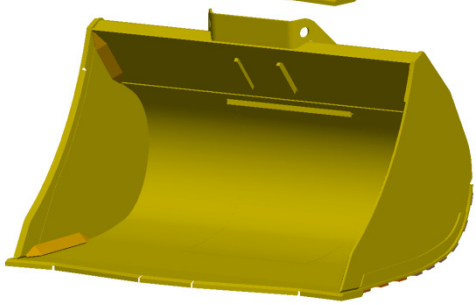

Figure 40: No base plate

Load	4970.5kg
Horizontal force per kg load	14.9N/kg
Vertical force per kg load	-3.3N/kg
Horiz. force compared to normal	-6.4%

Bucket without base plate, but with the wrapper moved inwards to keep constant volume, did not decrease horizontal force. A logical result is generated for bucket without base plate and a larger volume.

4.2.4 Side Plate Profile

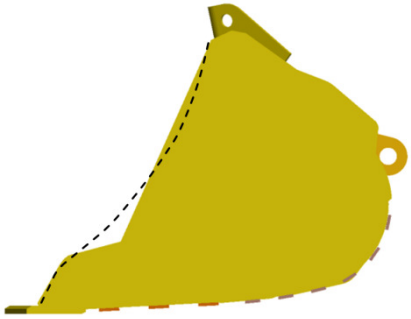

Figure 41: Side profile 1

Load	4711.8kg
Horizontal force per kg load	16.2N/kg
Vertical force per kg load	-3.0N/kg
Horiz. force compared to normal	-2.7% *

* Due to design, compared to normal bucket with flat side plates.

- - - - Normal side profile.

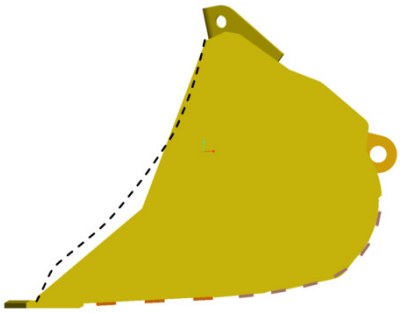

Figure 42: Side profile 2

Load	4660.5kg
Horizontal force per kg load	15.6N/kg
Vertical force per kg load	-3.3N/kg
Horiz. force compared to normal	-6.3% *

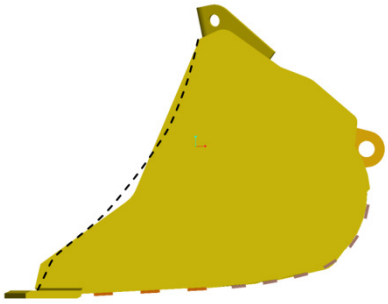

Figure 43: Side profile 3

Load	4710.8kg
Horizontal force per kg load	16.1N/kg
Vertical force per kg load	-3.0N/kg
Horiz. force compared to normal	+1.0%

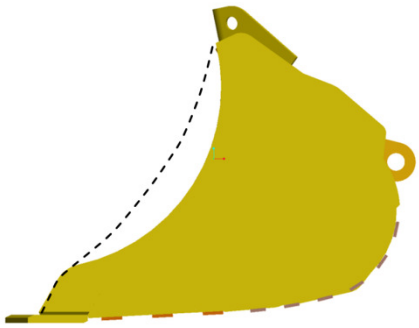

Figure 44: Side profile 4

Load	4602.5kg
Horizontal force per kg load	16.8N/kg
Vertical force per kg load	-2.6N/kg
Horiz. force compared to normal	+5.4%

Side plate profile with a more edgy shape in lower part decrease horizontal force compared to normal profile.

4.2.5 Support Plate

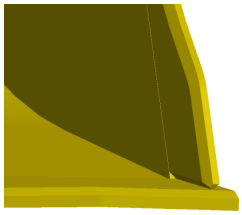

Figure 45: No support plate

Load	4775.0kg
Horizontal force per kg load	15,5N/kg
Vertical force per kg load	-3.8N/kg
Horiz. force compared to normal	-2.7%

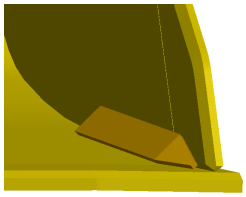

Figure 46: Support plate (GIII, Normal)

Load	4720.1kg
Horizontal force per kg load	15,9N/kg
Vertical force per kg load	-3.4N/kg
Horiz. force compared to normal	0.0%

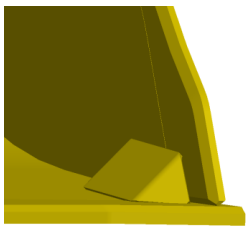

Figure 47: Large support plate

Load	4690.5kg
Horizontal force per kg load	16,3N/kg
Vertical force per kg load	-2.9N/kg
Horiz. force compared to normal	+2.5%

Smaller or no support plate give lower horizontal forces.

4.2.6 Edge Thickness

The bucket lip is 40mm thick. The standard shape is a chamfer angle of 30deg and an edge thickness of 25mm, see Figure 48.

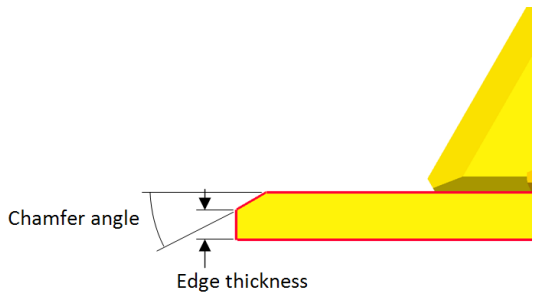

Figure 48: Chamfer angle and edge thickness.

Edge thickness 25mm (GIII, Normal)

Load	4720.1kg
Horizontal force per kg load	15,9N/kg
Vertical force per kg load	-3.4N/kg
Horiz. force compared to normal	0.0%
Horiz. force comp. - high setup	0.0%

Edge thickness 8mm

Load	4763.0kg
Horizontal force per kg load	15.0N/kg
Vertical force per kg load	-0.8N/kg
Horiz. force compared to normal	-5.7%
Horiz. force comp. - high setup	-6.8%

A thinner edge has a large impact on horizontal force.

4.2.7 Lip Chamfer Angle

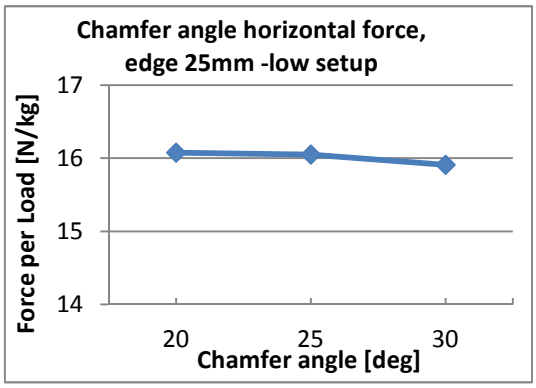

Figure 49: Chamfer angle plotted against horizontal force for lip with 25mm thickness.

For a bucket with edge thickness 25mm the chamfered area is small and no difference in forces can be distinguished between chamfer angles.

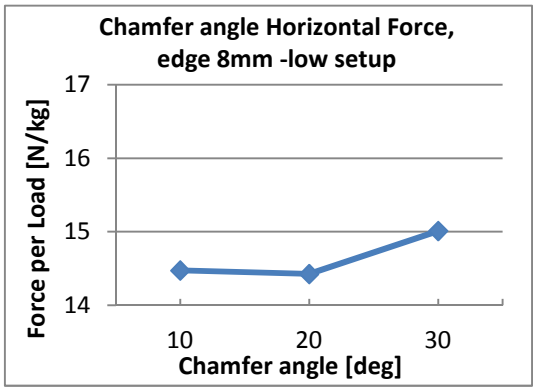

Figure 50: Chamfer angle plotted against horizontal force for lip with 8mm thickness, low setup.

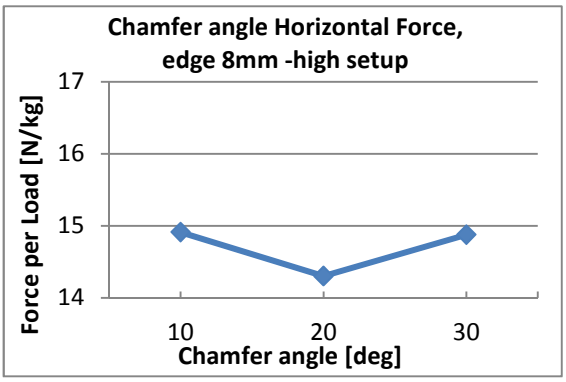

Figure 51: Chamfer angle plotted against horizontal force for lip with 8mm thickness, high setup.

For buckets with edge thickness 8mm the chamfer area is larger and differences are distinguished. Chamfer angle of 20deg generates lowest horizontal forces for both high and low setup.

4.2.8 Lip Angle

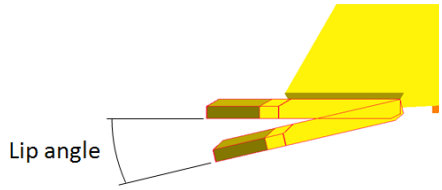

Figure 52: Lip angle

Positive angle value tilts the lip downwards.

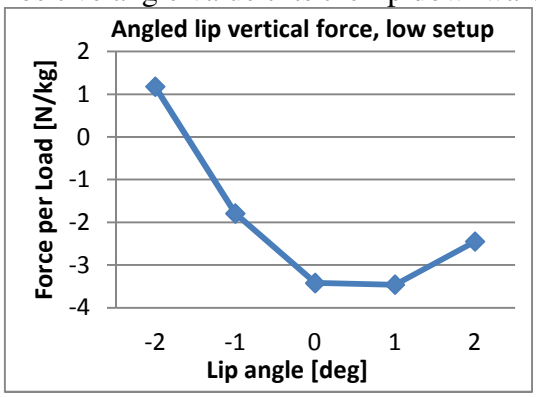

Figure 53: Vertical forces for angled lip.

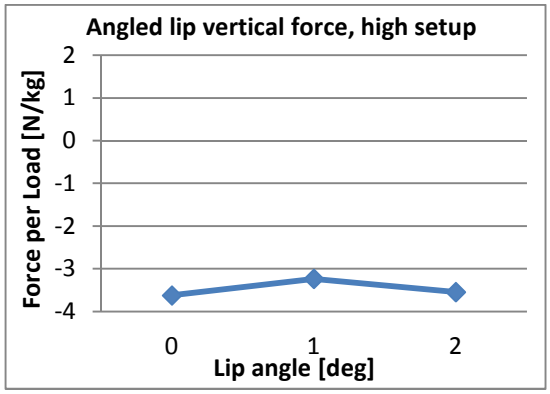

Figure 54: Vertical forces for angled lip, high setup, see Figure 24.

The vertical force vector points upwards, a negative force is there for good due to better tire grip. Lip angle 0deg generates best vertical forces.

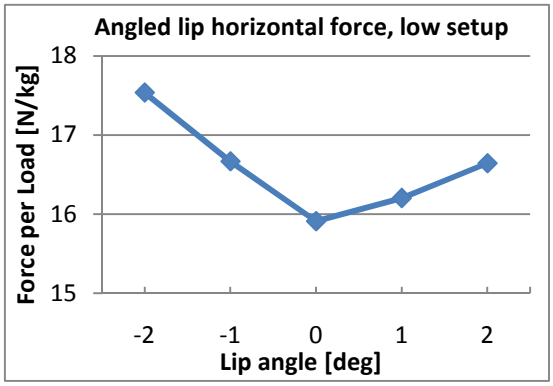

Figure 55: Horizontal forces for angled lip.

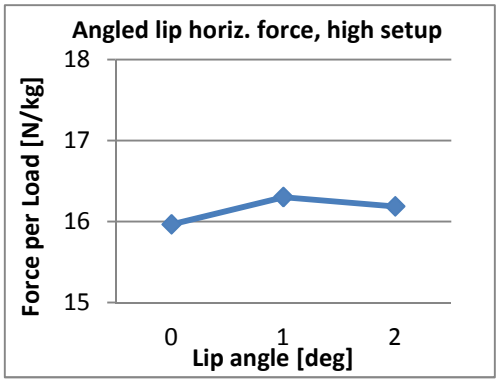

Figure 56: Horizontal forces for angled lip, high setup.

Horizontal forces were lowest for lip without angle.

4.2.9 Attack Angle

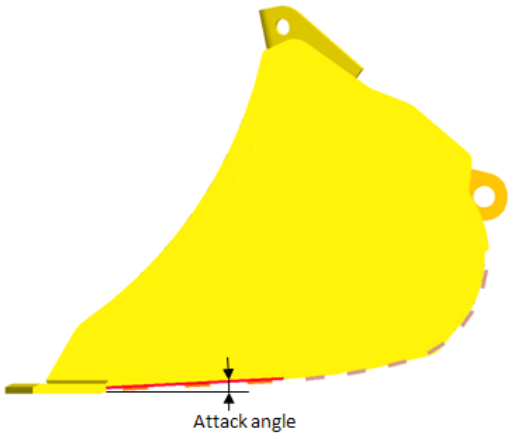

Figure 57: Attack angle

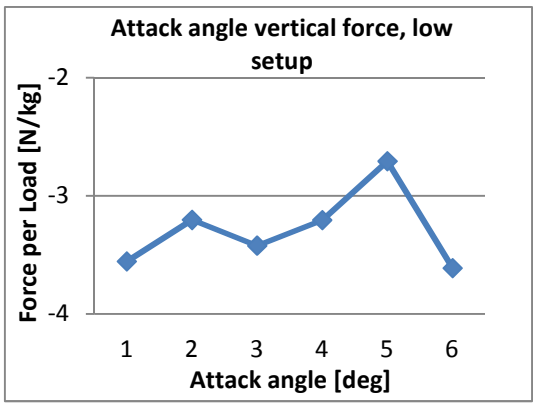

Figure 58: Vertical forces for attack angle, low setup.

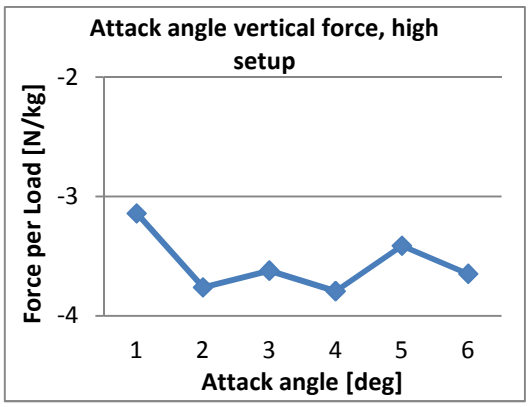

Figure 59: Vertical forces for attack angle, high setup.

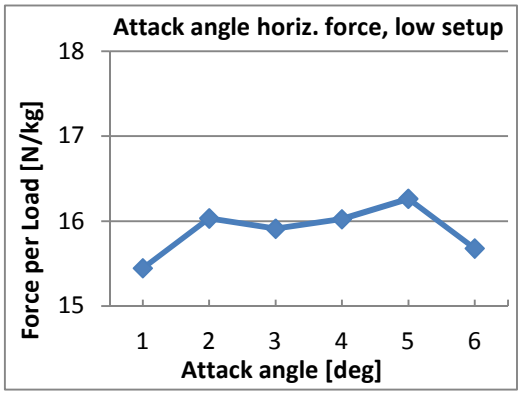

Figure 60: Horizontal forces for attack angle, low setup.

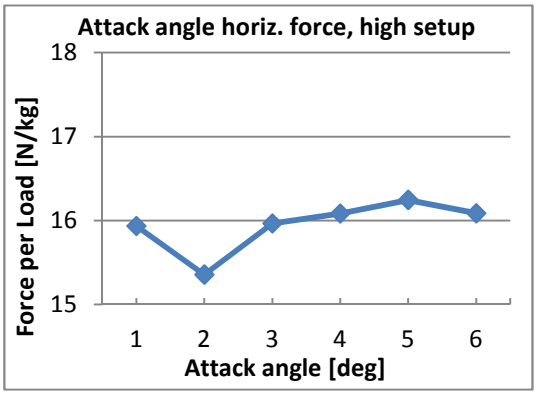

Figure 61: Horizontal forces for attack angle, high setup.

For both horizontal and vertical force it is difficult to distinguish a trend in relation to bottom angle.

4.2.10 Side Plate Angle

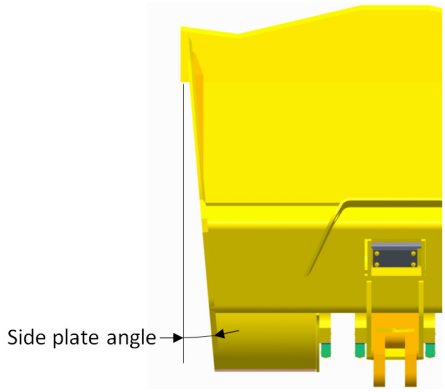

Figure 62: Side plate angle.

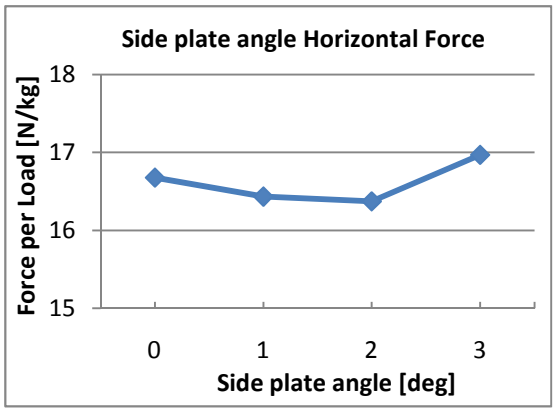

Figure 63: Horizontal forces for side plate angle.

Horizontal force is lowest for side plates with an angle of 1 and 2deg.

The outer side of the side plates were flat for all buckets in this test. Bucket with no angle of side plate but with a flat outer side had a 4.8% larger horizontal force compared to a normal bucket. A normal side plate has a reinforcement plate along the side profile.

4.2.11 GET

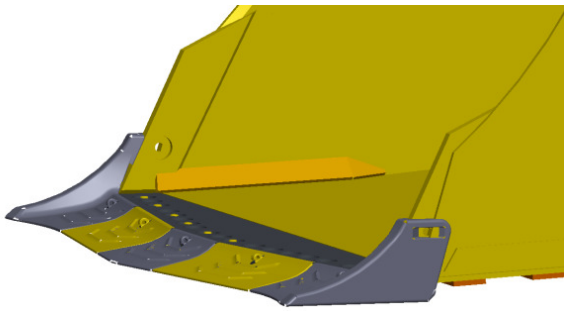

Figure 64: GET

Load	5065.5kg
Horizontal force per kg Load	14.3N/kg
Vertical force per kg Load	-4.1N/kg
Horiz. force compared to normal	-10.1%
Horiz. force comp. - high setup	-7.0%

GET (Ground Engagement Tools) is a new lip under development at Atlas Copco. The lip consists of five exchangeable plates made of high strength steel. As seen in Figure 64 the lip has a thin edge compared to normal lip. The buckets loading capacity is larger due to a longer lip. This lip shape generates the lowest horizontal force of all buckets.

Atlas Copco's own field tests have shown an increased loading efficiency of about 10% for this bucket.

5 Conclusions

5.1 Practical Test

The worse result for the GII bucket is believed to be related to a couple of differences in the design.

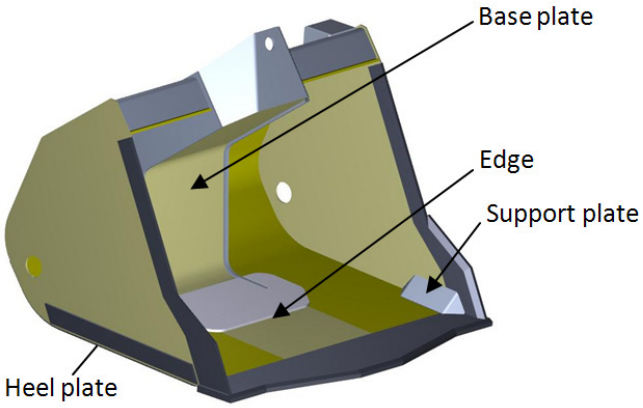

Figure 65: GII bucket with design differences.

The upper part of base plate interact more with the material. An edge from a reinforcement plate in the bottom adds resistance to material flow. As shown in chapter 4.2.5 the larger support plate increase horizontal force. A heel plate is mounted underneath the GII bucket, not visible in **Fel! Hittar inte referenskälla.**, this plate adds a friction force when it is in contact with material. The GIII bucket is slightly wider than the GII bucket, this can make the GIII bucket easier to fill.

An factor that add some insurance to the test was the more worn tires on the GII machine, which could give the machine a lower tractive force.

5.2 Investigating the Influence of Design Parameters

5.2.1 GII Bucket

As the practical test showed GII bucket is more difficult to fill also in the simulation setup. See chapter 5.1 above.

5.2.2 Lip Profile

Overall the differences in horizontal forces are small and it difficult to draw conclusions from the result. The hypothesis was that a more edgy shape were going to generate lower forces, an explanation to that this wasn't seen more clearly can be related to that small angles are used, larger angles will decrease usability.

V/straight lip did have a lower horizontal force than the normal GIII Bucket, for both high and low cycle. This small change would probably also decrease wear on lip corners which is critical.

5.2.3 Base Plate Profile

A bucket without base plate but with the wrapper moved inwards to keep constant volume,

Figure **39**, did not decrease the horizontal force. This even increased horizontal force by 1.7%. To verify the result a normal bucket without base plate was tested and the

forces for this bucket did decrease. From the result of this test there is no reduction in horizontal force when replacing base plate by moving the wrapper inwards.

Compared to a bucket without base plate but with constant volume, the base plate get into contact with the material earlier but the wrapper plate in the pockets get into contact with the material later. This generates only a small difference between the two buckets.

5.2.4 Side Plate Profile

The lower part of the side plate has most interaction with loading material and the design of this part is there for important. Side plate profile 2 has a sharp shape in the lower part and this is the reason to why the horizontal force is lower for this profile. The bad result for profile 4 partly depends on the reduction in loaded material for that design.

From the test with thinner edge thickness of the lip it was shown that a thinner edge largely reduces the forces. This can also be applied on the side profile edges, but this has not been confirmed by tests.

5.2.5 Support Plate

The result shown for different support plate design was logical, the forces increase with larger support plates. The difference of 2.7% without support plate is that large that a design without support plate is motivated to prioritize.

By having a smoother angle in the end closest to the lip, forces may be reduced without deleting the support plates

5.2.6 Edge Thickness

The edge thickness has a large influence on horizontal force; a thinner edge generates a smaller horizontal force. From the test this is seen as the most important design parameter.

5.2.7 Lip Chamfer Angle

A logical result for the chamfer angle is that the horizontal force decreased for lower angles, which give a sharper edge. For an edge thickness of 8mm a chamfer angle of 20deg had lowest horizontal forces for both high and low setup. This is probably related to simulation variation and it is risky to conclude that a chamfer angle of 20deg is better than 10deg. But it could at least be seen that the difference between 10deg and 20deg has a negligible effect on horizontal force.

For a lip with 25mm edge thickness the chamfer area is small and the chamfer angle has a low influence on the forces.

5.2.8 Lip Angle

A horizontal lip was shown to generate lowest horizontal force. The hypothesis was that an lip angled downwards were going to increase vertical force and improve tire grip, this wasn't shown in neither high or low simulation setup.

5.2.9 Attack Angle

In the result for different attack angles no readable trend was distinguished. The hypothesis was that a large angle was going to generate higher vertical forces but that wasn't shown. The result did coincide with the study performed by Maciejewski [7],

see Figure 10 and Figure 11. For a rotational loading motion the attack angle has a small influence on forces. Without rotation a high attack angle will increase the horizontal force.

5.2.10 Side Plate Angle

An side plate angle of 1 and 2 deg showed lowest forces in this test. But all buckets in the side angle test showed a higher horizontal force than the standard bucket. This was because the buckets used in the side angle test had a flat outer surface. The normal GIII bucket has reinforcement plates along the edge which adds a gap of 20mm to the rear part of the side plate, see Figure 66. This gap creates the same clearance as an angled plate, but without adding an angle inside the bucket which decrease the volume and increase friction forces.

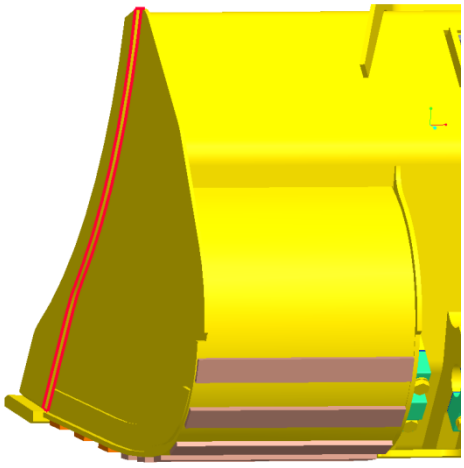

Figure 66: Gap from reinforcement plate highlighted.

5.2.11 GET

The GET Bucket showed lowest horizontal force of all buckets in the test. The explanation to this is seen clearly when individual design parameters on the GET bucket is studied. A thin edge thickness has been shown to be the individual most important parameter and on the GET bucket the edge thickness is 7mm. The side plates continues on the lip sides and has a sharp angle, this design is shown to be efficient in

Figure **42**.

6 Discussion

6.1 Reflections on EDEM

From the beginning a realistic material was the goal to generate. In the first simulation setup the particles flow path was the dominating factor on the result. This gave a large result variation and it was hard to distinguish how individual design parameters did influence the result. The particles used had 5-spheres and an edgy shape and also a large size variation. To decrease the influence from the particle flow path on the result a more smooth material was created. The particles shape was changed to the one shown in Figure 16. This particle only consist of 3-spheres bonded close together, the particles where also smaller with a lower size variation.

Even if this new material wasn't the most realistic one it was able to produce a readable result. The same problem appears in reality when buckets are tested, the particles flow path will have a large influence on the result.

6.2 Recommendations

To increase the reliability in the simulations more accurate settings are recommended to use, but this will largely increase simulation time. By simulating with a shorter timestep the simulations will be more reliable. Multiple runs with the same bucket will generate the same result and force peaks will be reduced. To compensate for that different particle flow paths not is generated with this setup the recommendation is to create multiple piles with the same kind of particles and outer size, but with an internal difference of the particles placement in the pile. By simulating each bucket design in 10 different piles with a shorter timestep for both low and high setup, the accuracy and reliability in the simulation would increase.

Other improvements to make are to improve simulation material and build a model of the motion in ADAMS to get a more realistic movement of the bucket.

For future simulations larger design changes are recommended to study and different bucket sizes.

7 References

7.1 Literature

1. Atlas Copco (2010): *Atlas Copco annual report 2009,* Atlas Copco AB, Stockholm, Sweden, 2010
2. Atlas Copco (2008): *Mining Methods in Underground mining, Third edition.* Linder U, Atlas Copco AB, Örebro, Sweden, 2008
3. Coetzee C J, Basson A H, Vermeer P A (2006): *Discrete and continuum modelling of excavator bucket filling*, Journal of Terramechanics, No 44 , 2007, 177–186 pp.
4. Coetzee C J, Els D N J (2007): *The numerical modelling of excavator bucket filling using DEM.* Journal of Terramechanics No 46, 2009, 217–227 pp.
5. Esterhuyse SWP (1997) *The influence of geometry on dragline bucket filling performance.* M.Sc. Thesis Mechanical Engineering, University of Stellenbosch, Stellenbosch, South Africa.
6. Jing L, Stephansson O (2007): *Fundamentals of Discrete Element Methods for Rock Engineering, Theory and Applications*. Elsevier, Amsterdam, Netherlands, 2007, 7-14 pp.
7. Maciejewski J, Jarzcebowski A (2002): *Laboratory optimization of the soil digging process*, Journal of Terramechanics, No 39, 2002, 161–179 pp.
8. Nezami E, Hashash Y, Zhao D, Ghaboussi J (2006): *Simulation of front end loader bucket–soil interaction using discrete element method,* International Journal for Numerical and Analytical Methods in Geomechanics, No 31, 2007, 1147-1162 pp.
9. Rowlands JC (1991): *Dragline bucket filling*. Ph.D Thesis, University of Queensland, Queensland, Australia.
10. Takahashi H (1999): *Analysis on the Resistive Forces acting on the Bucket in Scooping Task of Piled Fragment Rocks by Use of Distinct Element Method.*
11. Torres R. (2008): *Soil-bucket interaction, A new approach*, Master Thesis. Department of Aeronautical and Vehicle Engineering, Kungliga Tekniska Högskolan, Stockholm, Sweden
12. Zhao D, Nezami E, Hashash Y, Ghaboussi J (2006): *Three-dimensional discrete element simulation for granular materials*, International Journal for Computer-Aided Engineering and Software, No 7, 2006

7.2 Internet Sources

13. Atlas Copco (2007), Atlas Copco Wagner Inc, timeline and milestones, viewed 16 Feb 2010, <http://www.atlascopco.com.au/auus/news/productnews/timeline__milestones.asp>
14. ESSS (2009), EDEM Case: Simulation of Iron-ore transportation viewed 18 March 2010, <http://www.dem-solutions.com/ugm/proceedings/pdf/2009-EDEMUGM-%20Spogis.pdf>

15. RoyMech (2009), Friction Factors, viewed 18 March 2010, <http://www.roymech.co.uk/Useful_Tables/Tribology/co_of_frict.htm>

7.3 Interviewees

16. Lars Bergqvist - Senior Advisor - Mining, Atlas Copco
17. David Curry - Ph.D. CAE, DEM Solutions
18. Totte Nilsson - Machine Operator, Atlas Copco
19. Morgan Norling - Senior MBS Analyst, Atlas Copco
20. Stefan Nyqvist - Mechanical Designer, Atlas Copco
21. Erik Svedlund - Product Manager, Atlas Copco

A Appendix

A1 Technical Specification ST7

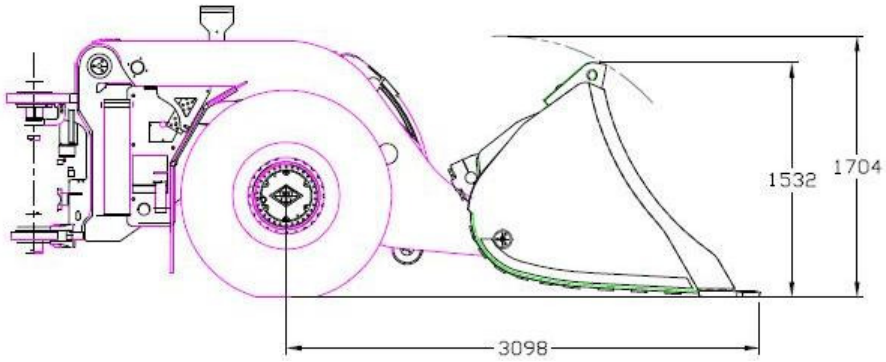

Figure 67: Profile picture ST7 GIII standard Bucket.

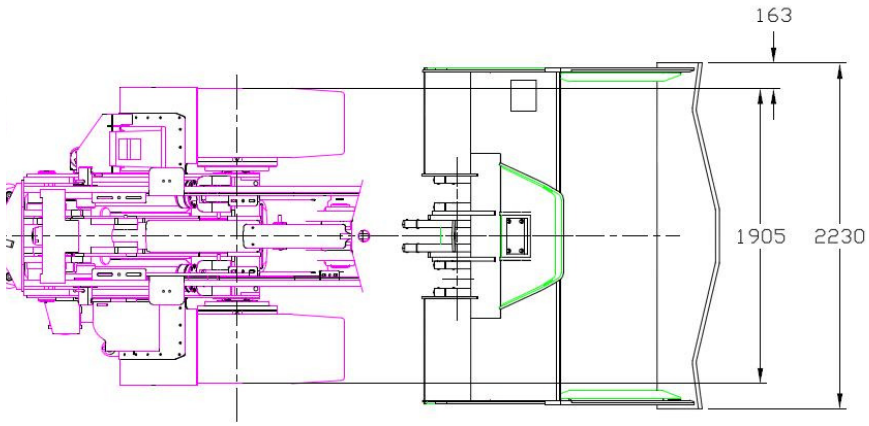

Figure 68: ST7 GIII standard bucket from above.

Table 2: ST7 specification.

Length	8.62m
Width (vehicle)	2.12m
Height	2.16m
Tramming capacity	6 800kg
Weight	19 300kg
Engine power	193hp
Breakout force (mechanical)	13 900kg

Tramming Capacity 6800kg

The maximum weight the machine is able to carry is fixed. Since the density of the rock varies between mines the size of the bucket differs. For more heavy rock the buckets are smaller. The standard bucket is made for a material density of 2,2t/m³ and has a volume of 3,1m³.

Breakout Force (mechanical) 13 900 kg

The breakout force is the force produced by the dump cylinder which gives the tilting motion to the bucket. It is measured 100mm in from the bucket tip. The force is mechanical limited since the rear wheels are losing the ground contact at 13 900kg. The hydraulic limitation is 15 200kg.

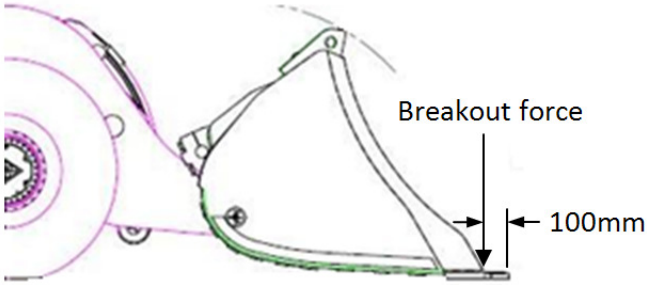

Figure 69: Breakout force description.

Engine Power 193hp

Atlas Copcos loaders have four wheel drive. The engine power is divided between the drive line and the hydraulic pump. This gives a reduced tractive effort when the bucket is in motion by the hydraulics, e.g. when it is tilted.

Tractive Effort 150kN

The maximal tractive effort for the ST7 machine, measured on concrete floor with full bucket, is 150kN, at 2200rpm [19]. In real tests a rough estimation of the maximal tractive effort during the loading cycle was 120kN (1800rpm). For relation between tractive effort and rpm, see Figure 70. An exact tractive effort is hard to calculate since it is dependent of the grip of the wheels, the wheel diameter and the amount of the engine power used for the hydraulic pressure.

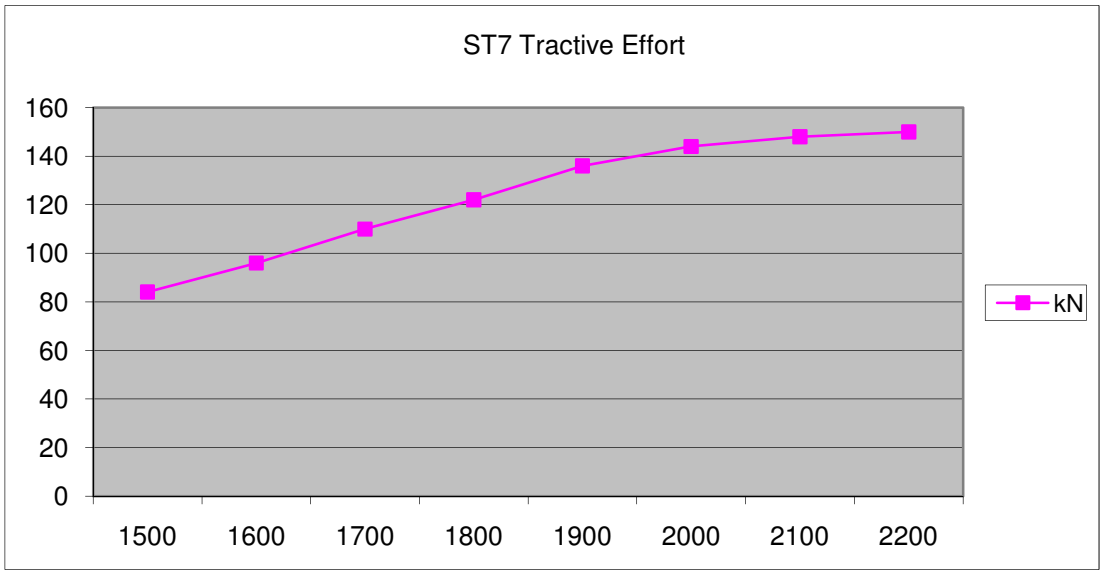

Figure 70: Tractive effort in kN related to rpm for ST7.

A2 Mining Process

The most appropriate mining process to use in a mine is dependent of the shape of the orebody. Since the shape of orebodies never looks exactly the same, the most effective mining method is individual for each mine.

The different mining methods can be divided into two main groups based on the dip of the orebody, those two groups are described on next page. There exist also several additional variants of both methods.

Mining in steep orebodies

Where the dip exceeds 50 degrees, mining method for steep orebody is applied. The blasted material gravitate to a collection level where loading and main hauling are carried out, see Figure 71.[2]

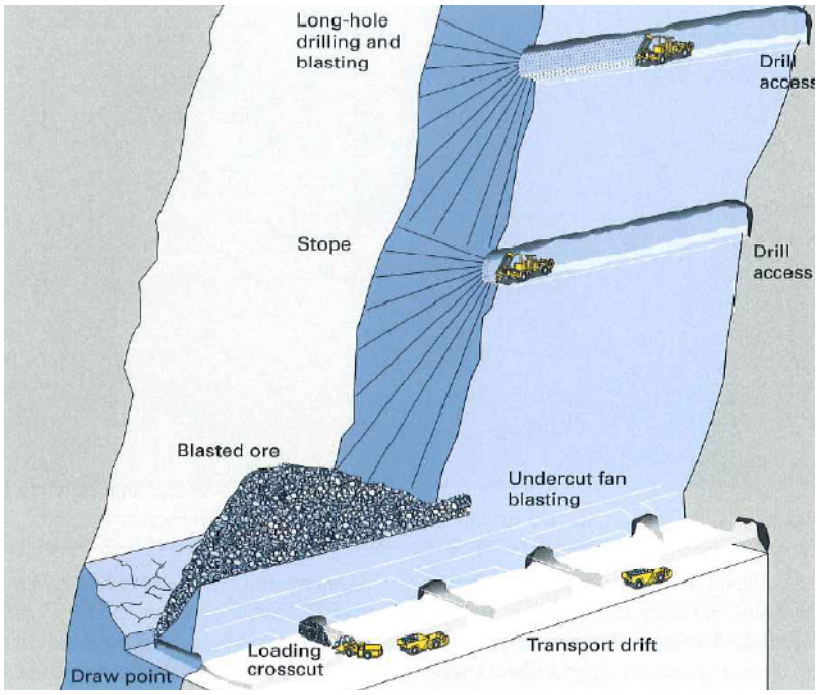

Figure 71: Mining in steep orebodies.

Mining in flat orebodies

In flat orebodies there are pillars left to support the structure from falling together. With this method the loading is taking place at the same place as the blasting.[2]

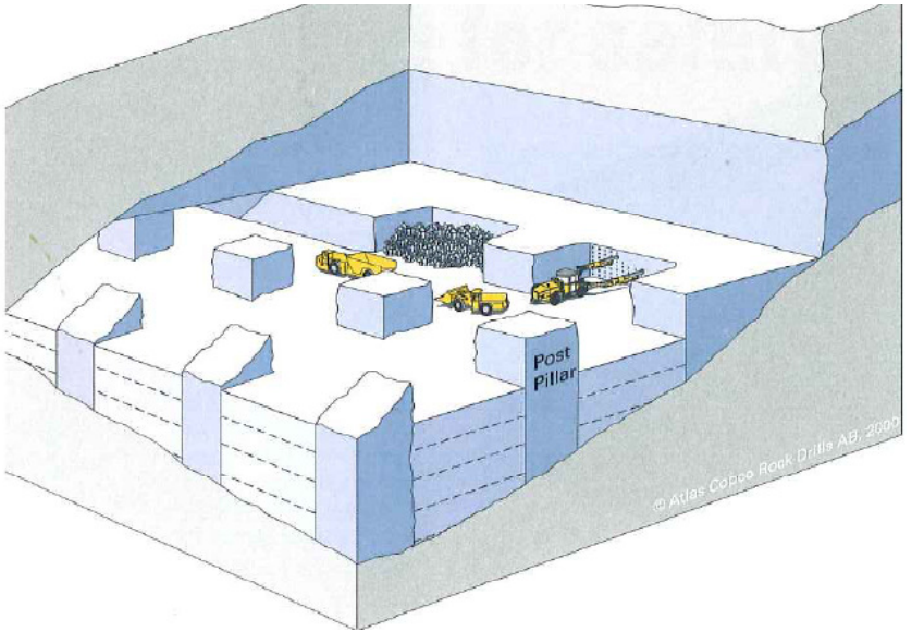

Figure 72: Mining in flat orebodies.

In mining methods for steep orebodies material is stored above the loading pile which compresses the material. This makes the rock piles from steep orebodies harder to penetrate with the bucket compared to the piles from flat orebodies.

A3 Bucket Motion in EDEM

Table 3: Bucket motion specified in EDEM.

Translational motion					**Rotational motion**		
		Horizontal	Horiz. acc.	Vertical			
	Time [s]	[m/s]	[m/s²]	[m/s]		Time [s]	[deg/s]
1	0-1.5	0.5			1	1.5-3	1.33
2	1.5-7.5	0.32			2	3-6	3.33
3	7.5-9	0.53		0.033	3	6-7.5	8
4	9.75-10.125		-5		4	7.5-9	16
5	10.125-10.5	-1.875			5	9-9.375	4

A4 Force Graphs GIII

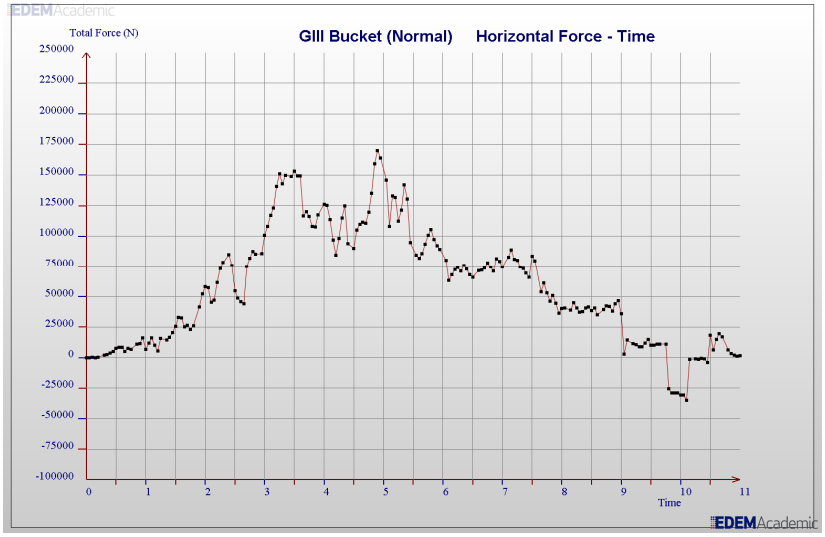

Figure 73: Graph of horizontal force on GIII bucket.

In Figure 73 it can be seen how the horizontal force increase when bucket digs into the pile. After 5s the rotational motion is large enough to make the force decrease.

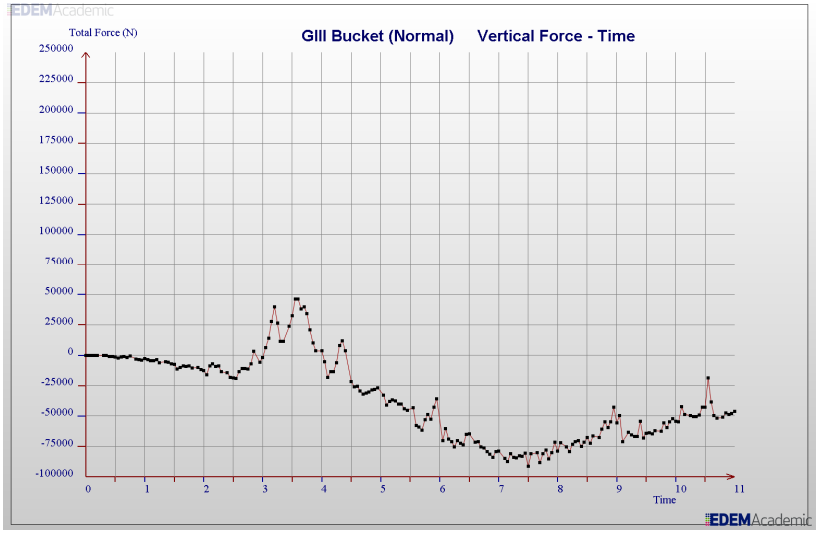

Figure 74: Graph of vertical force on GIII bucket.

Between 3 and 4s the vertical force on the bucket points upwards, this is probably a simulation error due to particles high compression forces.